Olanzapine manipulates neuroactive signals and may onset metabolic disturbances

Pukar Khanal, Farshid Zargari, Yadu Nandan Dey & Zahra Nikfarjam

Published online: 21 Jul 2023.

Submit your article to this journal ⬈

View related articles ⬈

View Crossmark data ⬈

Taylor & Francis
Taylor & Francis Group

Check for updates

Olanzapine manipulates neuroactive signals and may onset metabolic disturbances

Pukar Khanal[a]*[#] (iD), Farshid Zargari[b,c]*, Yadu Nandan Dey[d] (iD) and Zahra Nikfarjam[e]

[a]Department of Pharmacology, NGSM Institute of Pharmaceutical Sciences (NGSMIPS), Nitte (Deemed to be University), Mangalore, India; [b]Pharmacology Research Center, Zahedan University of Medical Sciences, Zahedan, Iran; [c]Department of Chemistry, Faculty of Science, University of Sistan and Baluchestan, Zahedan, Iran; [d]Department of Pharmacology, B.C. Roy College of Pharmacy and Allied Health Sciences, Durgapur, India; [e]Department of Physical Chemistry, Chemistry and Chemical Engineering Research Center of Iran, Tehran, Iran

Communicated by Ramaswamy H. Sarma

ABSTRACT

Olanzapine is one of the most prescribed atypical antipsychotics to treat psychiatric illness and is associated with weight gain and metabolic disturbance. The present study investigated the olanzapine-regulated metabolic pathways using functional enrichent analysis including binding affinity with G-protein-coupled receptors (GPCRs). Proteins modulated by olanzapine were retrieved from SwissTargetPrediction, DIGEP-Pred, and BindingDB and then enriched in Search Tool for the Retrieval of Interacting Genes/Proteins (STRING) to assess molecular function, biological process, and cellular components including Kyoto Encyclopedia of Genes and Genomes (KEGG) pathways. We used homology modeling to improve the 3D structure for GPCR synapse proteins including dopamine, serotonin, muscarinic, and histamine receptors which were then optimized using molecular dynamics (MD) simulations. The protein-olanzapine binding mechanisms for different GPCR binders were evaluated using molecular docking; later refined by MD simulations. Binding mechanism of olanzapine with D2, 5HT1A, 5HT2A, 5HT2B, 5HT2C, M1, and M2 receptors were created using homology modeling and optimized using MD simulations. In target identification, it was observed that olanzapine majority targeted G-protein coupled receptors. Further, enrichment analysis identified around 76% of the total genes regulated in molecular function, biological process, and cellular components were common including KEGG pathways. Moreover, it was observed that olanzapine had a major potency over the neurotransmitter synapse including neuroactive signals . Olanzapine-induced weight gain and metabolic alterations could be due to the deregulation of multiple synapses like dopamine, serotonin, muscarinic, and histamine at the feeding center followed by cGMP-PKG, cAMP, and PI3K-Akt signaling pathways.

HIGHLIGHTS

- Olanzapine is used in the management of psychiatric illnesses.
- Olanzapine causes disturbance in lipids and glucosehomeostasis and manipulates energy expenditure.
- Olanzapine-induced weight gain may occur due to the deregulation of the multiple synapse and cGMP-PKG, cAMP, and PI3K-Akt signaling pathway

CONTACT Yadu Nandan Dey ✉ yadunandandey@gmail.com 🖃 Department of Pharmacology, Dr. B. C. Roy College of Pharmacy and Allied Health Sciences, Durgapur-713206, West Bengal, India
*Equal contribution and treated as the first authors.
#Department of Pharmacology and Toxicology, KLE College of Pharmacy Belagavi, KLE Academy of Higher Education and Research (KAHER), Belagavi 590010, India.
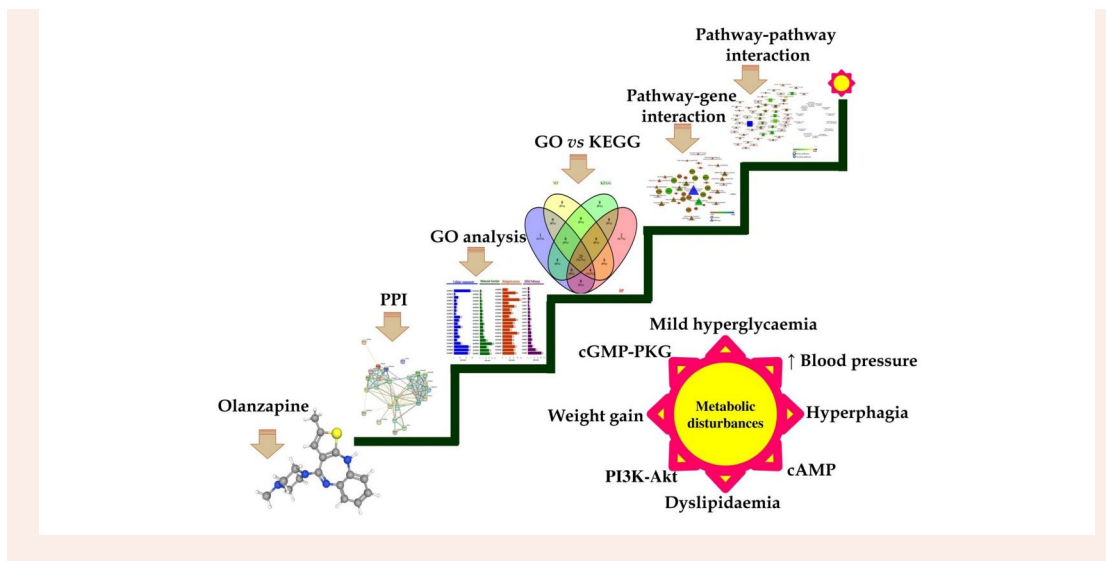
Introduction

Olanzapine, one of the atypical antipsychotics covers the majority portion of the prescription in the management of psychiatric illnesses including schizophrenia (Narasimhan et al., 2007). Although it has importance to treat psychotic illness it is well recognized for inducing weight gain which has been successfully reported in the subjects undergoing olanzapine pharmacotherapy and experimental rat animal models and zebrafish (Khanal et al., 2020; Lord et al., 2017).

Multiple investigations have been made to understand olanzapine-induced obesity in which hyperphagia and compromised ATP utilization or energy expenditure followed by mild sedation are in trend (Fernø et al., 2011; Ullagaddi et al., 2021). However, the conditions observed in the experimental animal models are quite interesting i.e. dose-dependent, gender-dependent, and strain-dependent; primarily focused female Sprague Dawley animal models at the dose of 2 mg/kg bid (Albaugh et al., 2006; Patil et al., 2006). Also, a report has been made to compromise the catabolism of the lipid and metabolic rate due to the exposure of olanzapine; demonstrated in the olanzapine-exposed zebrafish larvae and enhanced food intake in adult zebrafish (Khanal et al., 2020).

Additionally, olanzapine-induced weight gain is one of the popular animal models in investigating anti-obese drugs primarily targeting the subjects under the pharmacotherapy of olanzapine-induced weight gain (Hu et al., 2014; Parasuraman et al., 2017; Ullagaddi et al., 2021). However, since the mechanism of olanzapine-induced obesity is not well established, it becomes quite problematic in proposing the mechanism of action of their anti-obese drugs as the targets affected by the inducing agent i.e. olanzapine remains unclear for obesity. Hence, it is an important aspect to evaluate the primarily regulated pathways and their association with multiple proteins and pathways via olanzapine is in need. In this regard, the present studyaimed to investigate the association of olanzapine in modulating multiple proteins and their linkage with various pathways in obesity through functional enrichment analysis based on the theory of 'a single compound can regulate multiple proteins'.

Methodology

Identification of olanzapine-regulated/binding targets

The SMILES of olanzapine was retrieved from the PubChem database (https://pubchem.ncbi.nlm.nih.gov/) and their targets were predicted in SwissTargetPrediction; (Gfeller et al., 2014; http://www.swisstargetprediction.ch/); probability **0.5**, DIGEP-Pred; (Lagunin et al., 2013; http://www.way2drug.com/ge/); pharmacological activity **0.5**, and BindingDB which were a public, web-accessible database of measured binding affinities for biomolecules, genetically or chemically modified biomolecules, and synthetic compounds; (Liu et al., 2007; https://www.bindingdb.org/bind/index.jsp); probability **0.7** and the codes of each protein were retrieved from UniProt database (https://www.uniprot.org/). The regulated and binding proteins were further overlapped with proteins reported for obesity concerning the DisGeNET database (Piñero et al., 2017; https://www.disgenet.org/) concerning the *C0028754* entry.

Functional enrichment analysis

The regulated and binding proteins were then enriched in Search Tool for the Retrieval of Interacting Genes/Proteins (STRING; Szklarczyk et al., 2019; https://string-db.org/) *ver*. 11.0 for *Homo sapiens* for functional enrichment analysis to evaluate the molecular function, targeted cellular components, and multiple biological spectra followed by Kyoto Encyclopedia of Genes and Genomes (KEGG; https://www.genome.jp/kegg/) metabolic pathways. The network was constructed using Cytoscape (Shannon et al., 2003; https://cytoscape.org/) *ver* 3.5.1. The constructed network was treated as directed and evaluated using the edge count variable. The node size was directly proportional to the edge count. Additionally, the common interaction of gene ontology terms and KEGG-associated genes were analyzed using Venny 2.0; (Oliveros, 2007–2015; https://bioinfogp.cnb.csic.es/tools/venny/).

Table 1. Models for each protein were created using accessible crystal structures.

Protein name	PDB ID (Chains)	Ligand
5-hydroxytryptamine receptor 1 A (5HT1A)	7E2X (R), 7E2Y (R), 7E2Z (R)	SRO, 9SC
5-hydroxytryptamine receptor 2 A (5HT2A)	6A93 (A), 6A94 (B), 6WGT (A), 6WH4 (C), 6WHA (A)	89F
5-hydroxytryptamine receptor 2B (5HT2B)	4IB4 (A), 4NC3 (A), 5TUD (A), 5TVN (A), 6DRX (A), 6DRY (A), 6DRZ (A), 6DS0 (A)	H8J
5-hydroxytryptamine receptor 2 C (5HT2C)	6BQG (A), 6BQH (A)	ERM
D(2) dopamine receptor (DRD2)	6LUQ (A), 6CM4 (A), 6VMS (R)	08Y
Muscarinic acetylcholine receptor M1 (CHRM1)	5CXV (A), 6OIJ (R), 6WJC (A)	0HK
Muscarinic acetylcholine receptor M2 (CHRM2)	5ZKC (A), 4MQS (A), 5ZK3 (A), 6OIK (R), 6U1N (R), 4MQT (A), 5ZK8 (A)	2CU

Homology modeling of proteins

Using the crystal structures from the protein data bank (PDB) as templates, the homology modeling tool Modeller 7v7 (Martí-Renom *et al* 2000; Sali & Blundell 1993; Fiser et al., 2000) was used to create a reliable 3D homology model for each protein. The ligand and PDB codes with maximum similarity with olanzapine were summarized (Table 1). Later the proteins were prepared for molecular docking and molecular dynamic (MD) simulations. The respective ligand was used for active site determination in the docking study.

Molecular docking and MD simulation setup

Since the interaction of olanzapine with the aforementioned proteins and their linkage with various pathways are vital and effective in biochemical and biological processes, a molecular docking protocol was followed to trace a stable ligand-protein complex (Morris & Lim-Wilby, 2008). Molegro Virtual Docker (http://molexus.io/molegro-virtual-docker/) and UCSF Chimera (https://www.cgl.ucsf.edu/chimera/download.html) were used to prepare the structures, including hydrogen addition and energy minimization (Pettersen et al., 2004). Ledock packages that use simulated annealing-genetic crossover algorithm for conformational search, and docking scoring covers van der Waals interaction, electrostatic interaction, hydrogen bond contribution, as well as intermolecular and intramolecular ligands, were used to perform molecular docking simulations. (Liu & Xu 2019). The substrate-binding pocket residues were covered by the grid box (Jin et al., 2020). The binding site of olanzapine for each receptor set according to the geometrical position of ligands was reported (Table 1) for each receptor. The optimal position (Figure 1) with the highest negative binding affinity was recorded once the docking process was completed. The superior pose with the appropriate binding orientation was chosen for MD simulation and binding free energy computation. A molecular dynamic simulation was used to account for the ligand-receptor complex's dynamic and solvent effects.

A parallel version of PMEMD from the Amber 20 program was used to carry out the MD simulations. To generate the input for each receptor, we first introduced the receptor to orientations of proteins in membranes (OPM) server (Lomize et al., 2012; https://opm.phar.umich.edu/) for spatial arrangements of membrane proteins concerning the hydrocarbon core of the lipid bilayer (Figure 1). The output of the OPM server for each receptor was used to construct the MD simulation input using CHARMM-GUI server v 3.7 (Jo et al., 2008). In the CHARMM-GUI server, we used CHARMM general force field to treat the ligand topology file. The protein orientation was along the Z-axis in a rectangular box type with a water thickness of 22.5 Å. We used the heterogeneous lipid bilayer with ratios of lipid components as 2:2:1 for POPC: POPE: Cholesterol lipids. The Amber input file was generated using the AMBERff14SB force field surrounded by the OPC water model (Izadi et al., 2014). The periodic boundary condition (PBC) was applied in all three dimensions. The ligands' force field parameters were internally converted to the GAFF using the CHARMM-GUI server. The system was cleared of erroneous interconnections using an energy reduction strategy that involved 2500 steepest-descent steps followed by 2500 conjugated-gradient stages, with the head group of lipids and the backbone atoms of proteins being strategically restricted. At 303 K, a series of NVT was ensembled with a Langevin thermostat for 120 ps to perform releasing of the restraints from protein and lipid. Likewise, a series of NPT simulations propose to use Berendsen barostat with semi-isotropic coupling with enabled surface tension in XY planes for 2 interlaces again releasing the restraints from protein and lipid. Long-range electrostatics were controlled using the particle mesh Ewald (PME) method. The SHAKE algorithm was used to restrict all covalent bonds, including hydrogen atoms. A nonbonded cutoff of 9.0 Å was used, allowing for a 2 fs time step. The MD simulation (300 ns) was performed for each protein-ligand complex.

MMPBSA/MMGBSA for entropy correction to calculate the complex binding free energies

Biomolecules' interactions with their environment determine the structure, dynamics, and functions of biomolecular systems. Explicit and implicit solvent models can simulate solvent-solute interactions. These models require high computing power to sample and model the interactions of individual atoms in water and solute molecules. Implicit solvent models concentrate on short-term performance and monitoring while attempting to simulate mean-field solute and solvent interactions. Implicit models function admirably and consistently in many biological applications, but they are less precise (Wang et al., 2016). A number of widely used implicit models are based on the Poisson-Boltzmann (PB) equation, which characterizes polar solvation interactions as classical electrostatic interactions. In this study, the Molecular Mechanics Poisson-Boltzmann Surface Area (MMPBSA) technique was used to predict protein-ligand binding interactions using PB-based solvent models, particularly when combined with explicit solvent. Similar to the MMPBSA method, binding affinities can be affected by changes in solvation, electrostatic and VDW interactions, and other factors (Wang et al., 2016). The molecular mechanics energies paired with the Poisson-Boltzmann surface area (MM/PBSA) or generalized Born surface area (MM/GBSA) as continuous solvation methods are recognized methodology for
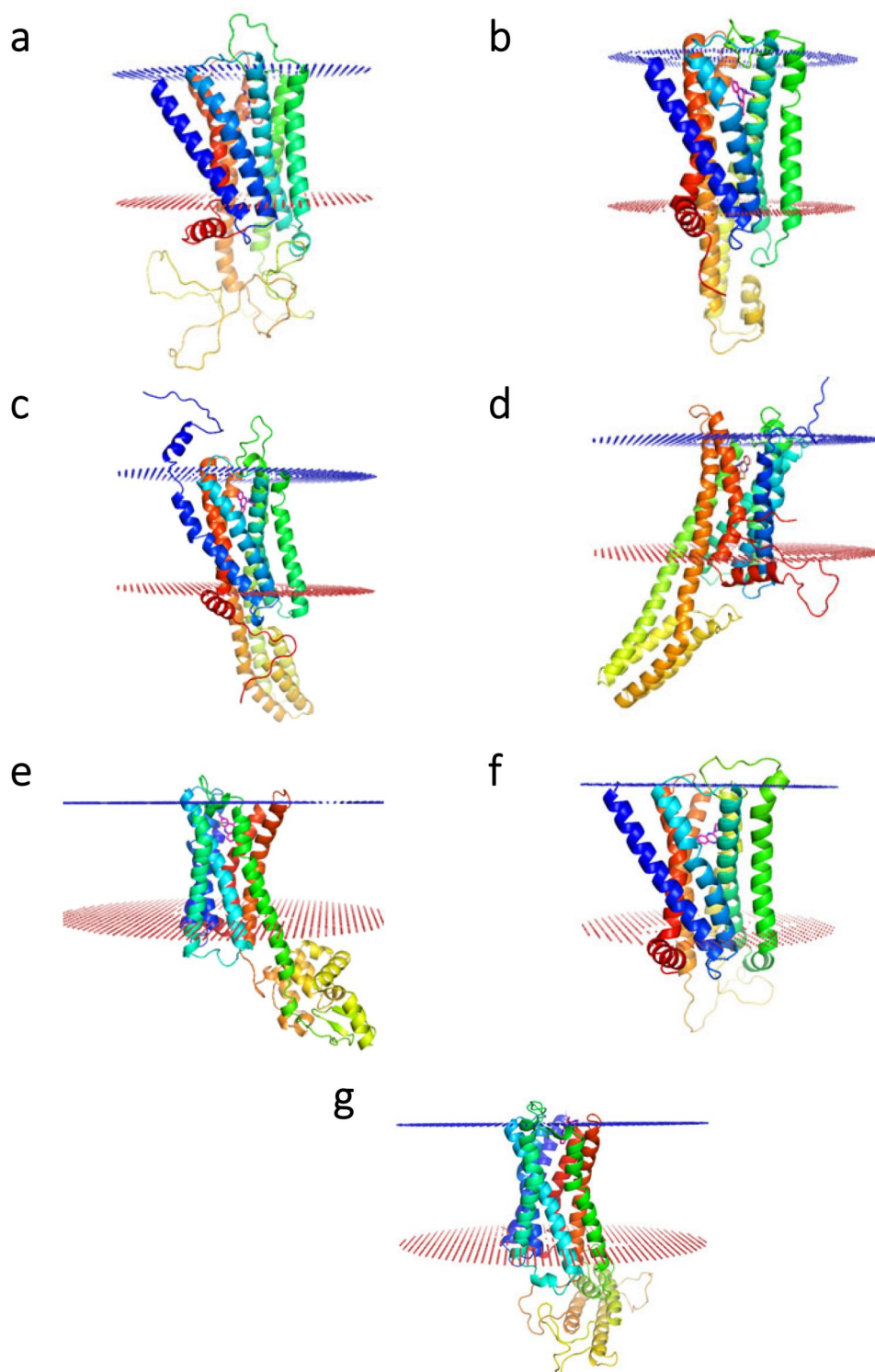
Figure 1. Binding mode of olanzapine bound to the (a) 5HT1A, (b) 5HT2A, (c) 5HT2B, (d) 5HT2C, (e) DRD2, (f) CHRM1, and (g) CHRM2 obtained from docking.

determining the binding free energy of minute ligands to biological macromolecules.

Normal mode analysis is commonly used to calculate entropy (NMA). Due to their acceptable accuracy, relatively low computational cost, and widely applicable scopes, such as for small-ligand-protein systems, protein-protein systems, and protein–RNA/DNA systems, MM/GBSA and MM/PBSA have become the most popular methods for large-scale binding free energy calculations in the last decade(Chang et al.,

2016; Hou & Yu, 2007; Sun et al., 2013; VARGiu & Magistrato, 2012; Wang et al., 2001). Entropy effects play a crucial role in drug-target interactions, influencing the binding affinity between ligands and their target proteins. However, incorporating entropy calculations, particularly through normal mode analysis (NMA), poses computational challenges due to its high computing cost. As a result, widely used end-point binding free energy calculation methods such as MM/GBSA and MM/PBSA often simplify the calculations and overlook
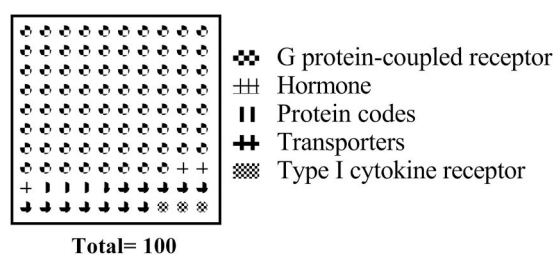
Figure 2. Categories of proteins regulated by olanzapine. Olanzapine was majorly identified to act on G-protein coupled receptors followed by transporters including type 1 cytokine receptors, protein codes, and hormones.
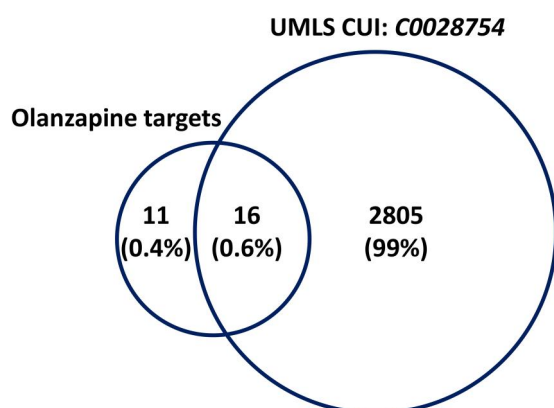

Figure 3. Association of olanzapine-regulated targets with obesity (DisGeNET entry: C0028754). a total of 16 (0.6%) olanzapine-modulated proteins were observed to overlap with obesity; C0028754.

the explicit consideration of entropic contributions to ligand-binding affinity. This omission is primarily due to the trade-off between computational cost and the lower prediction accuracy associated with NMA. Consequently, many applications utilizing MM/GBSA and MM/PBSA methods commonly disregard the entropy change associated with protein-ligand binding. Nonetheless, a variety of strategies have been used to accurately estimate entropy, ranging from post-processing approaches (Ben-Shalom et al., 2017; Genheden et al., 2012) to simulation-synchronized methodologies. For example, Genheden et al. demonstrated that using truncated structures for the NMA entropy calculation could be a viable strategy for reducing processing costs. The same group also discovered that, aside from NMA, most entropy estimate approaches fail to converge even with very long simulation times i.e. 1 ms, (Genheden et al 2014; Genheden & Ryde, 2012) limiting their practical application. The binding free energy was calculated using the recently established entropy calculation method i.e. called interaction entropy (Duan et al., 2016; Sun et al., 2018). The absolute binding free energy of a complex is computed using the MM/GBSA method by averaging the total gas-phase energy, solvation-free energy, and entropic contributions over many snapshots selected from the main MD trajectory. For determining the polar component of solvation-free energy, a grid-based surface GB model is combined with a novel water model and atomic radii proposed earlier in.

The absolute binding free energy, ΔG_{bind}, of a ligand L to a biomacromolecule, such as a protein, P, creating a complex PL is estimated using the MM/GBSA method. It calculates ΔG_{bind} as the free energy difference between PL (Protein-Ligand called Complex), P (Protein), and L (Ligand), i.e.

$$\Delta G_{bind} = G(PL) - G(P) - G(L) \ldots \ldots \quad (1)$$

The following sum is used to estimate each of these three free energies

$$G = E_{int} + E_{vdw} + E_{ele} + G_{solv} + G_{np} - TS_{MM} \ldots \ldots \quad (2)$$

The first three primary points on the right-hand side of the energy calculation include van der Waals, electrostatic energies, and internal molecular mechanics (MM) contributions, which account for bonds, angles, and dihedrals. In addition to these components, the final energy calculation incorporates the product of the absolute temperature and an estimated entropy term, which represents the contribution of molecular flexibility to the overall energy. Furthermore, the calculation includes terms for vibration, rotation, and translation. These factors are all calculated on a system where water molecules have been removed. It is important to note that in our simulations, we typically focus on the complex (PL), and the free energies of the protein (P) and ligand (L) are determined within the same simulation by excluding the coordinates of the other species (Foloppe & Hubbard, 2006; Swanson et al., 2004). In addition, in the present work, we employed MM/GBSA implemented in AmberTools22 (Case et al., 2022) for the binding free energy calculation.

Clustering and energy decomposition analysis

The clustering method is employed as a practical computational intelligence approach to effectively categorize MD frames into functionally homogeneous groups, enabling efficient identification of distinct sets. This method utilizes a superficial similarity score to partition each MD frame into multiple groups. By considering specific factors, MD frames within the same group can be compared to one another. By applying the clustering method to our MD data, we aim to unveil underlying patterns and discern functionally relevant conformations. This enables us to gain insights into the dynamic behavior of the ligand-receptor complex and identify functionally distinct states or conformations. The most common and well-known measure of similarity is the root mean square deviation (RMSD) values used for sorting MD trajectories derived by pairwise or matrix error distances (De Paris et al 2015). Further, if simulation data produces a representational structure, cluster analysis can be used to identify structural groups. Data points within a cluster are more comparable to data points outside the cluster when using clustering as a data-splitting approach. Before getting solid results using cluster analysis, there is typically a lot of trial and error required. (Nikfarjam et al., 2021). The breakdown of residues offers information about favorable and unfavorable interactions, which can help to improve lead quality. This study looked at the Water Swap residue-by-residue binding energy decompositions to see which residues contributed the most to inhibitor binding during the MD simulation (Kiani et al., 2019).
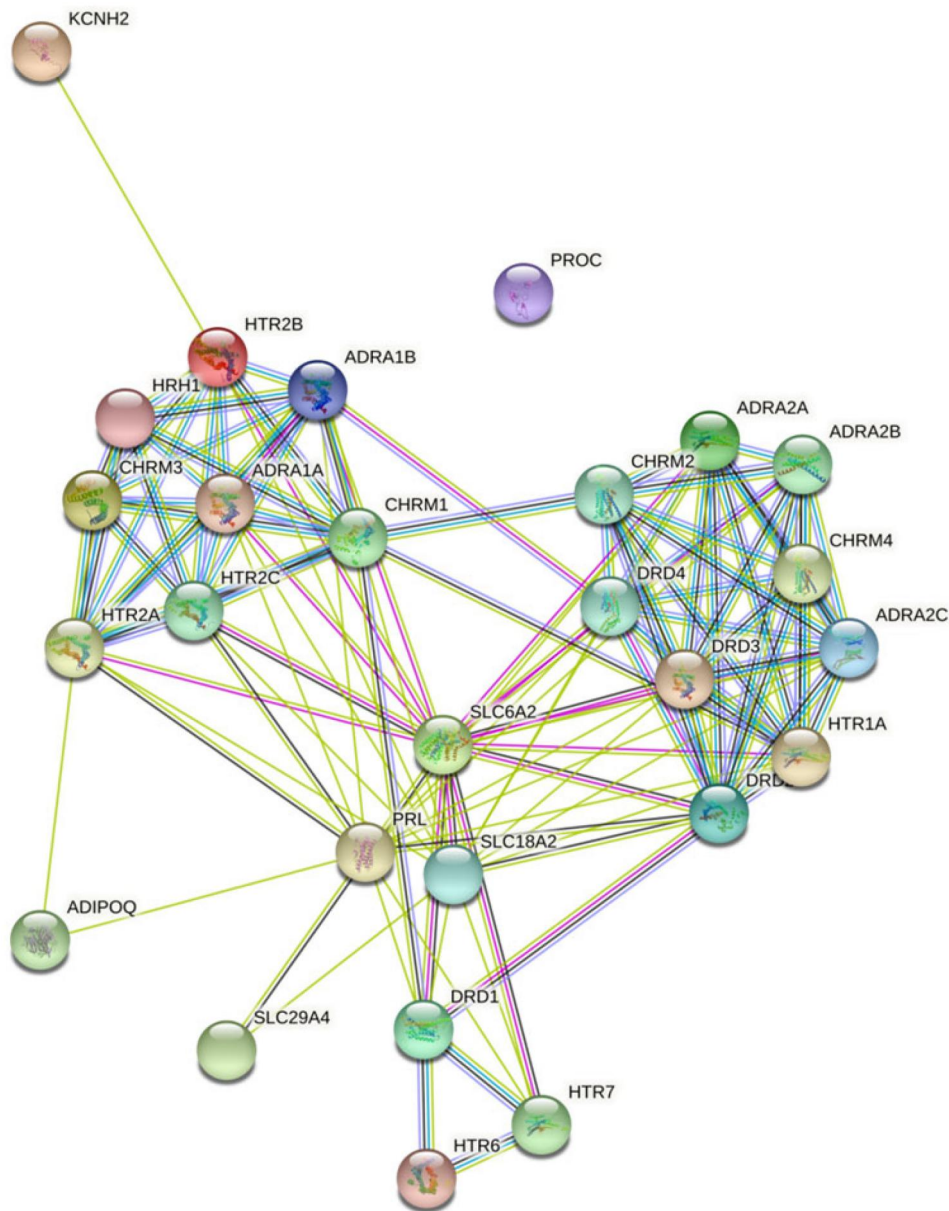
Figure 4. Protein-protein interaction of olanzapine-modulated targets. Node color; ⬤ colored nodes: query proteins and first shell of interactors, ⬤ white nodes: second shell of interactors, Node content; ◯ empty nodes: proteins of unknown 3D structure, ⬤ filled nodes: some 3D structure is known or predicted, Known Interactions; ◯━◯ from curated databases, ◯━◯ experimentally determined, Predicted Interactions; ◯━◯ gene neighborhood, ◯━◯ gene fusions, ◯━◯ gene co-occurrence & Others; ◯━◯ text mining, ◯━◯ co-expression, ◯━◯ protein homology.

Results and discussion

Olanzapine targeted 27 proteins which were categorized under G-protein coupled receptor, hormones, protein codes, transporters and type 1 cytokine receptors including ADRA1A, CHRM1, CHRM2, and DRD2 . Among the regulated proteins, G-protein coupled receptors were majorly modulated i.e. 78.125% (Figure 2). Similarly, 59.25% of the olanzapine-regulated proteins were in common with pre-identified targets for obesity concerning DisGeNET (entry: *C0028754*); Figure 3.

Enrichment analysis of the 27 olanzapine-regulated and binding proteins was predicted to interact with each other via 118 edges with an average node degree of 8.74, an average local clustering coefficient of 0.715, expected edge count of11 with a p-value of 1.0e-16 (Figure 4).

The olanzapine-regulated protein interaction-associated gene ontology terms were observed to link with KEGG pathways via the common involvement of 23 genes affecting a total effect of 76.7% (Figure 5). Gene ontology analysis predicted Cholinergic Receptor Muscarinic 2 (CHRM2) to be chiefly modulated by 18 gene ontology terms of a cellular component. In this, the integral component of the plasma membrane (GO:0005887) was chiefly modulated by regulating 23 genes against 1564 background proteins at the strength and false discovery rate of 1.03 and 1.16E-19 respectively (supplementary file; sheet 1). Likewise, in the molecular function, dopamine receptor D2 (DRD2) was

primarily modulated within 15 gene ontology molecular functions. Within it, G protein-coupled amine receptor activity (GO:0008227) was chiefly modulated via the regulation of 16 genes against 48 background proteins at the strength and false discovery rate of 2.38 and 4.74E-32 respectively (supplementary file; sheet 2). Also, in the KEGG analysis, dopamine receptor D1 (DRD1) was chiefly modulated associating with 9 different pathways. In this regard, neuroactive ligand-receptor interaction (hsa04080) was primarily modulated via the regulation of 21 genes against 272 background proteins at the strength and false discovery rate of 1.75 and 2.23E-32 respectively (supplementary file; sheet 3). Further,

for biological processes, dopamine receptor D2 (DRD2) was chiefly modulated within 232 biological processes. Also, G protein-coupled receptor signaling pathway, coupled to cyclic nucleotide second messenger (GO:0007187) was identified as a primarily modulated biological process via the regulation of 16 genes against 206 background proteins at the strength and false discovery rates at 1.75 and 7.48E-22 respectively (supplementary file; sheet 4). The top 20 gene ontology terms for molecular function, biological processes, cellular components, and regulated KEGG pathways are presented in Figure 6. Also, it was observed that olanzapine-regulated pathways modulate other secondary pathways in which Neuroactive ligand-receptor interaction was identified to be interlinked with maximum pathways (Figure 7).

The docking study pointed the propensity of the olanzapine ligand to be found in the active site of various protein targets. The selectivity of the ligand chosen for binding at the M2 receptor active site was higher than that of other structures (Table 2), and the M1 receptor structure was associated with the lowest affinity for binding. Utilizing molecular dynamics simulations, it was further examined how the ligand is situated at the active site of every protein structure under study.

The olanzapine obtained from the last step of the screening from the docking step was further studied by MD simulation. The lack of suitable protein sampling, ligand validation, and scoring procedures limits the precision of the binding energies acquired from molecular docking investigations. Considering multiple challenges such as insufficient protein sampling, ligand validation, and scoring functions to precisely assess binding energy, the data from molecular docking using more precise approaches should be evaluated. Binding scoring functions still need to regain their capacity
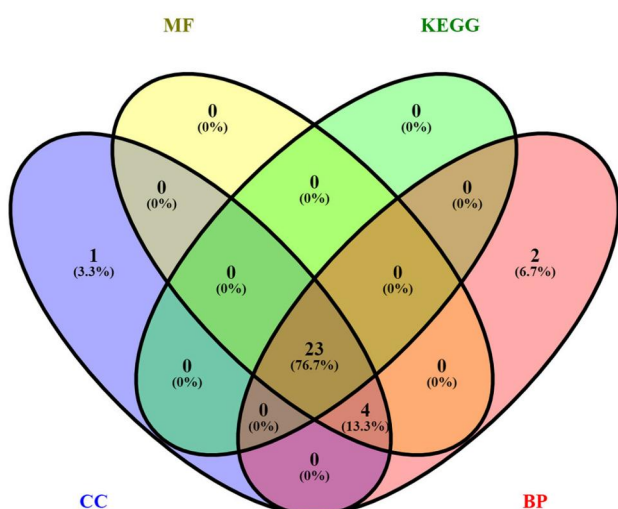

Figure 5. Interlinkage of cellular components, molecular function, biological processes, and KEGG pathways concerning pharmacological spectra of olanzapine-triggered proteins. *MF*: molecular function, *CC:* cellular components, *BP*: Biological processes, *KEGG*: Kyoto Encyclopedia of Genes and Genomes pathways.
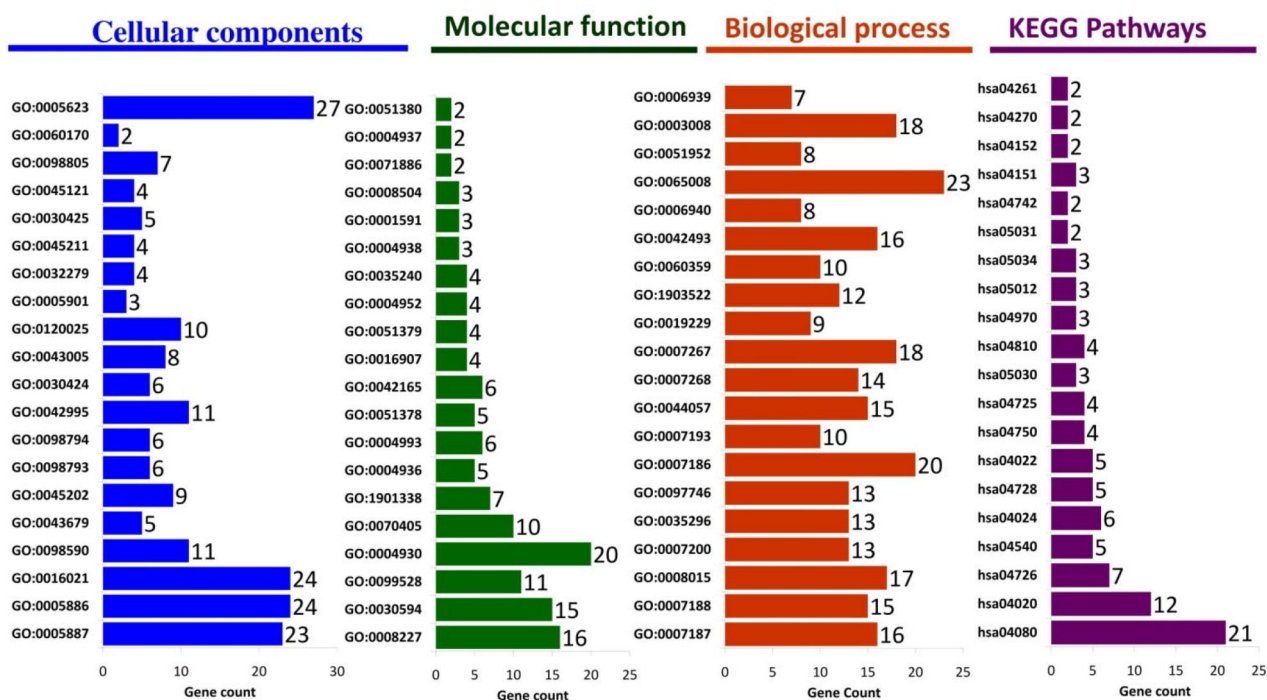

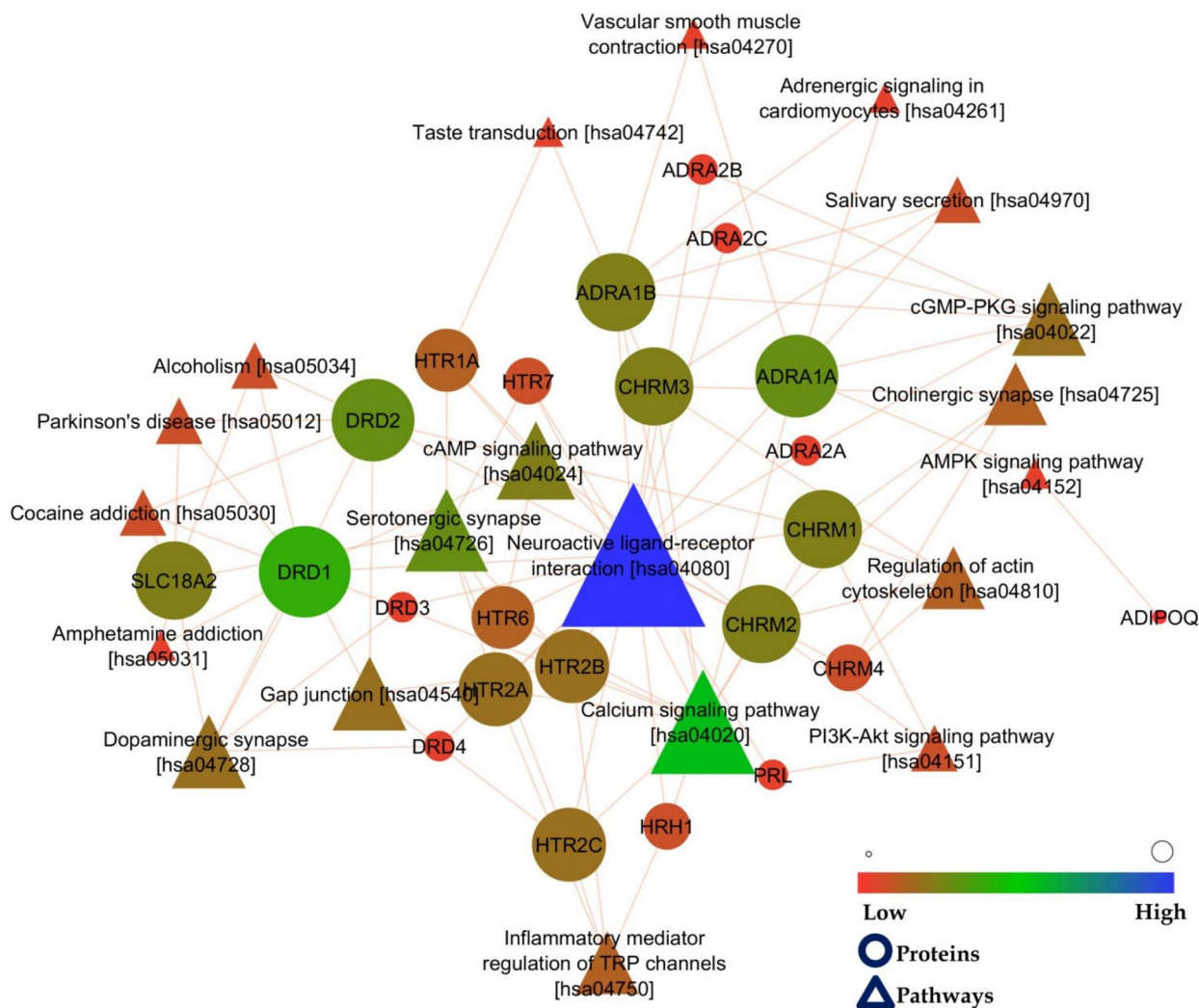Figure 6. Gene ontology analysis of olanzapine-modulated targets.

Figure 7. Olanzapine-regulated protein(s) interaction(s) with respective pathways. In the above interaction, the node size is directly proportional to the edge count.

Table 2. Docking of olanzapine ligand and selected receptors.

Receptor	Binding affinity (kcal/mol)
5HT1A	−5.24
5HT2A	−5.32
5HT2B	−4.99
5HT2C	−5.58
M1	−4.58
M2	−5.79
D2	−4.97

to rate binding and estimate free binding energies despite several attempts to improve their performance.

MM/PBSA and MM/GBSA are two methods that combine molecular mechanic energy and an implicit solvent model which are used in recognizing and ranking the accurate binding poses and ranking the inhibitors for specific targets (Nikfarjam et al., 2021; Shahraki et al., 2018). In this analysis, the best pose of olanzapine was simulated (300 ns) on the 7 selected targets. To calculate the MM-GB/PBSA binding energy, 1000 snapshots of MD pathways were obtained. Onufriev and Case created the modified GB model (igb = 5 dubbed GBOBC1) utilized in the GB calculations based on extensive tests and more agreement with the PB treatment
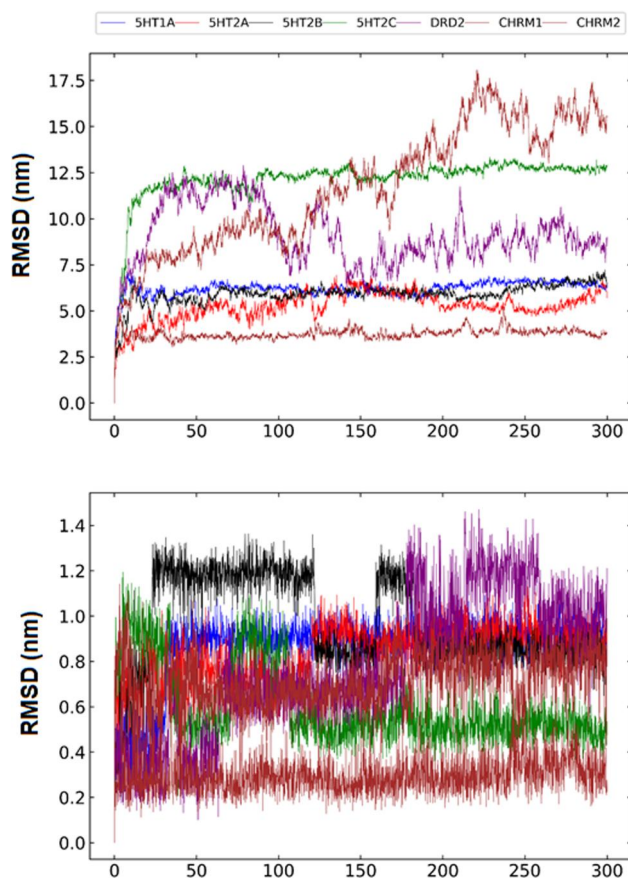
in calculating the electrostatic part of the solvation energy. The dielectric constant of the solute was fixed to one (Feig et al., 2004). As indicated the soltcon value was set to 0.15 M to reconcile the PB and GB solvation energies (Srinivasan et al., 1999).

The MM-PBSA/GBSA was calculated in the same way as presented in Table 3. By measuring solvent-free energies using the PB implicit solvent system, the non-polar solvent concept was obtained based on the solvent-accessible surface area (SASA) (Srinivasan *et al* 1999). To calculate the MM-PBSA binding energies of the ligands, the *istrng* was set to 15 mM, *radiopt* was set to 0, *fillratio* was set to 1.5, and the *indi* parameter was set to 4. The entropy was determined using the Amber *nmode* module using the 10 frames of MD simulation. These calculations incorporated a portion of the ligand from the previous snapshot.

The free energy generated from this procedure is summarized (Table 3). It's also worth noting that the data gathered through this approach converges statistically. For this category of ligands, the overall standard error is estimated to be around 1 kcal/mol. The classification of ligands has provided a more detailed picture. Given that the results

Table 3. Binding free energy of olanzapine bound to the GPCR receptors in the study.

	5HT1A	5HT2A	5HT2B	5HT2C	D2	M1	M2
ΔE_{VDW}	−39.43 ± 0.20	−32.30 ± 0.09	−44.00 ± 0.13	−40.27 ± 0.10	−28.90 ± 0.12	−46.39 ± 010	−36.88 ± 010
ΔE_{ele}	−0.18 ± 0.20	−5.97 ± 0.09	−8.04 ± 0.13	−5.07 ± 0.10	−3.92 ± 0.12	−3.17 ± 010	−8.02 ± 010
ΔE_{PB}	37.30 ± 0.20	23.48 ± 0.09	34.61 ± 0.13	28.92 ± 0.10	18.71 ± 0.12	26.95 ± 010	24.28 ± 010
ΔE_{NP}	−3.86 ± 0.20	−3.84 ± 0.09	−3.96 ± 0.13	−4.02 ± 0.10	−3.14 ± 0.12	−3.97 ± 010	−3.39 ± 010
ΔG_{solv}	33.42 ± 0.20	19.64 ± 0.09	30.65 ± 0.13	24.89 ± 0.10	15.56 ± 0.12	22.97 ± 010	20.88 ± 010
ΔG_{gas}	−39.62 ± 0.20	−38.27 ± 0.09	−52.05 ± 0.13	−45.35 ± 0.10	−32.82 ± 0.12	−49.56 ± 010	−44.91 ± 010
ΔG_{Bind}	**−6.18 ± 0.20**	**−18.63 ± 0.09**	**−21.39 ± 0.13**	**−20.46 ± 0.10**	**−17.26 ± 0.12**	**−25.58 ± 010**	**−24.02 ± 0.10**
ΔE_{VDW}	−39.43 ± 0.16	−32.30 ± 0.07	−44.00 ± 0.11	−40.27 ± 0.10	−28.90 ± 0.13	−46.39 ± 0.08	−36.88 ± 0.12
ΔE_{elec}	−0.18 ± 0.16	−5.97 ± 0.07	−8.04 ± 0.11	−5.07 ± 0.10	−3.92 ± 0.13	−3.17 ± 0.08	−8.02 ± 0.12
ΔE_{GB}	23.50 ± 0.16	24.45 ± 0.07	16.66 ± 0.11	13.12 ± 0.10	15.82 ± 0.13	20.75 ± 0.08	18.90 ± 0.12
ΔE_{Surf}	−4.61 ± 0.16	−4.16 ± 0.07	−5.34 ± 0.11	−5.07 ± 0.10	−3.84 ± 0.13	−5.24 ± 0.08	−3.82 ± 0.12
ΔG_{solv}	18.88 ± 0.16	20.29 ± 0.07	11.32 ± 0.11	8.04 ± 0.10	12.28 ± 0.13	15.51 ± 0.08	15.08 ± 0.12
ΔG_{gas}	−39.62 ± 0.16	−38.27 ± 0.07	−52.04 ± 0.11	−45.35 ± 0.10	−32.82 ± 0.13	−49.56 ± 0.08	−44.91 ± 0.12
ΔG_{Bind}	**−20.73 ± 0.16**	**−17.98 ± 0.07**	**−40.71 ± 0.11**	**−37.30 ± 0.10**	**−20.54 ± 0.13**	**−34.05 ± 0.08**	**−29.83 ± 0.12**
$T\Delta S_{total}$	−16.73 ± 3.10	−16.42 ± 3.07	−18.29 ± 1.59	−20.06 ± 1.07	−16.96 ± 3.20	−18.66 ± 1.20.	−17.57 ± 1.70
$\Delta G_{Bind,Entropy}$	**−3.93 ± 10.50**	**−1.56 ± 8.23**	**−22.95 ± 6.49**	**−16.81 ± 4.43**	**−3.97 ± 11.18**	**−15.66 ± 4.21**	**−11.52 ± 6.93**

Figure 8. RMSD Plots of protein backbone atoms of seven selected targets (up) and olanzapine (down) during 300 ns MD simulation.

Table 4. Analysis of hydrogen bond formation between olanzapine and selected targets.

Targets	Acceptor	Donor-H	Donor	Fraction	Distance
5HT1A	ASP82-O	OLZ-H13	OLZ-N5	0.0303	2.9
	ASP82-OD2	OLZ-H13	OLZ-N5	0.0103	2.9
	ASP82-OD1	OLZ-H13	OLZ-N5	0.009	2.9
	OLZ-N3	LYS156-HZ2	LYS156-NZ	0.005	2.86
	OLZ-N3	LYS156-HZ3	LYS156-NZ	0.005	2.86
	OLZ-N3	LYS156-HZ1	LYS156-NZ	0.0023	2.89
5HT2A	OLZ-N5	LEU155-HN	LEU155-N	0.0007	2.92
	ASP84-OD2	OLZ-H13	OLZ-N5	0.0007	2.92
5HT2B	ASP109-OD1	OLZ-H13	OLZ-N5	0.0037	2.87
	ASP109-OD2	OLZ-H13	OLZ-N5	0.0023	2.86
	OLZ-N4	ASN356-HD21	ASN356-ND2	0.002	2.95
5HT2C	ASP109-OD1	OLZ-H13	OLZ-N5	0.0037	2.87
	ASP109-OD2	OLZ-H13	OLZ-N5	0.0023	2.86
	OLZ-N4	ASN356-HD21	ASN356-ND2	0.002	2.95
M1	OLZ-N4	TYR249-HH	TYR249-OH	0.005	2.89
	OLZ-N3	ASN250-HD21	ASN250-ND2	0.0007	2.91
	OLZ-N2	TYR249-HH	TYR249-OH	0.0007	2.98
M2	PHE164-O	OLZ-H13	OLZ-N5	0.0963	2.9
	ILE161-O	OLZ-H13	OLZ-N5	0.037	2.88
	OLZ-N4	ASN390-HD21	ASN390-ND2	0.0153	2.941
	OLZ-N2	ASN390-HD21	ASN390-ND2	0.0047	2.94
D2	OLZ-N3	ARG70-HH11	ARG70-NH1	0.023	2.89
	TYR362-OH	OLZ-H13	OLZ-N5	0.0033	2.9
	ASP79-OD2	OLZ-H13	OLZ-N5	0.002	2.95
	ASP79-OD1	OLZ-H13	OLZ-N5	0.0013	2.87
	ARG70-O	OLZ-H13	OLZ-N5	0.0013	2.92

The RMSD profiles of the seven selected ligand-protein backbones (up) and specifically highlights the behavior of olanzapine (down) during the 300 ns MD simulation are illustrated (Figure 8). The corresponding findings provide insights into the ligand docking performance and reveals that olanzapine exhibits greater positional changes when bound to 5HT2B, followed by 5HT1A and 5HT2A receptors. These conformational changes allow the ligand to explore more favorable positions, potentially altering the ranking of binding energies obtained from the MMPBSA method (Table 3) compared to the initial docking analysis (Table 2). By elucidating the dynamic behavior of olanzapine and its influence on binding energy calculations, our study highlights the importance of considering protein stability in the presence of determinant compounds contributing to a better understanding of ligand-receptor interactions.

The hydrogen-bonding pattern for olanzapine with targets was also identified using hydrogen bonding analyses. Various portions of the ligand have formed a relative hydrogen bond

obtained from free energy are presented with entropy correction (Table 3). It can be seen that the tendency to bind olanzapine with two targets i.e. 5HT2C and M1 receptors was more than in other structures. This result will be discussed by further analysis.

The ligand binding efficacy to the receptor was evaluated using MD simulations. Various structural analysis methods, such as RMSD, decomposition analysis, and hydrogen bond assessment, were employed to characterize each ligand-protein interaction pattern. To estimate the ligand stability rescoring, a 300 ns MD study was conducted using the MMPBSA method.
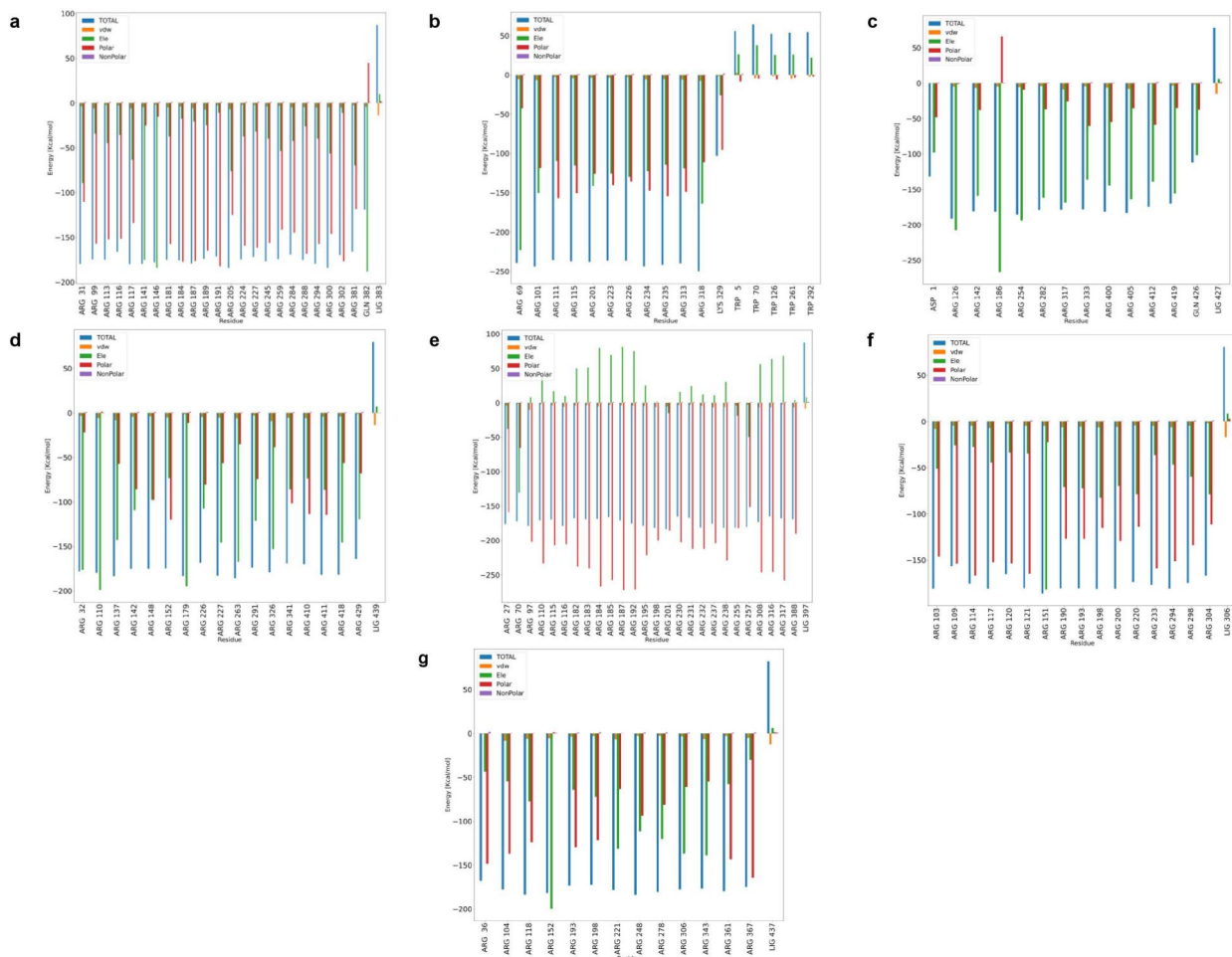
Figure 9. Energy decomposition analysis for the complexes between olanzapine with (a) 5HT1A, (b) 5HT2A, (c) 5HT2B, (d) 5HT2C, (e) DRD2, (f) CHRM1, and (g) CHRM2 through 300 ns molecular dynamics simulation.

with the residues Asp82 and Lys156 with the 5HT1A receptor (Table 4). Residues Asp109, Asn356, and Tyr382 have played an important role in the study of hydrogen bond analysis related to the structure of the 5HT2B receptor. Important residues related to this analysis concerning the structure of the 5HT2C include Asp120 and Ser124. Similarly, Tyr249 and Asn250 are significant residues in the M1 structure. Additionally, the structure of M2 facilitates the discovery of more efficient residues, such as Phe164, Ile161, and Asn390. The dopamine D2 receptor structure was effectively influenced by the residues Arg70, Tyr362, and Asp79. Because of the crucial residues in each target active site, it is apparent that the structures in hydrogen bond analyses revealed crucial hydrogen interactions with the olanzapine.

Further, we examined the decomposition analysis related to the complex of each target with olanzapine. Examining the analysis related to the target 5HT1A (Figure 9) it can be observed that the residues Arg31, Arg205, and Arg300 have the highest amount of total energy. Taking a closer look, we observed that the important electrostatic and van der Waals interactions related to residues Arg141, Arg146, and Gln396 were higher than other residues. Examining this analysis for the 5HT2A structure (Figure 9), we observed that residues Arg69, Arg101, and Arg318 had a high share of total energy. This was in the contribution of electrostatic and van der

Waals interactions related to residue Arg201. Important residues in relation to the 5HT2B target were Arg126, Arg186, Arg254, and Arg405. The range of relevant residues included Arg110, Arg137, Arg179, Arg263, Arg326, and Arg418 in 5HT2C played a key part in the van der Waals and electrostatic interactions. Even if some residues in the dopamine D2 receptor may not have the ideal level of electrostatic energy, van der Waals and other crucial interactions have made a sizable contribution. For this reason, in addition to residues of Arg70, Arg255, and Arg257; have total optimal energy, residues of Arg184, Arg187, Arg192, and Arg317 also had a significant share of intermolecular interactions. The study of decomposition analysis related to the structure of M1 showed that residues Arg103, Arg151, Arg190, Arg193, Arg294, and Arg304 could have played an effective role in total energy followed by detailed interactions. Similarly, M2 structure residues Arg36, Arg152, and Arg248 had a significant role in creating a proper interaction with the selected ligand (Figure 9). The significance of this approach was to consider if the olanzapine ligand locates in the protein's active site or not during 300 ns of molecular dynamics simulations. It can be confirmed that the target was appropriate for the investigated ligand if the ligand is more thoroughly positioned at the active regions of proteins by forming more stable connections with more residues.
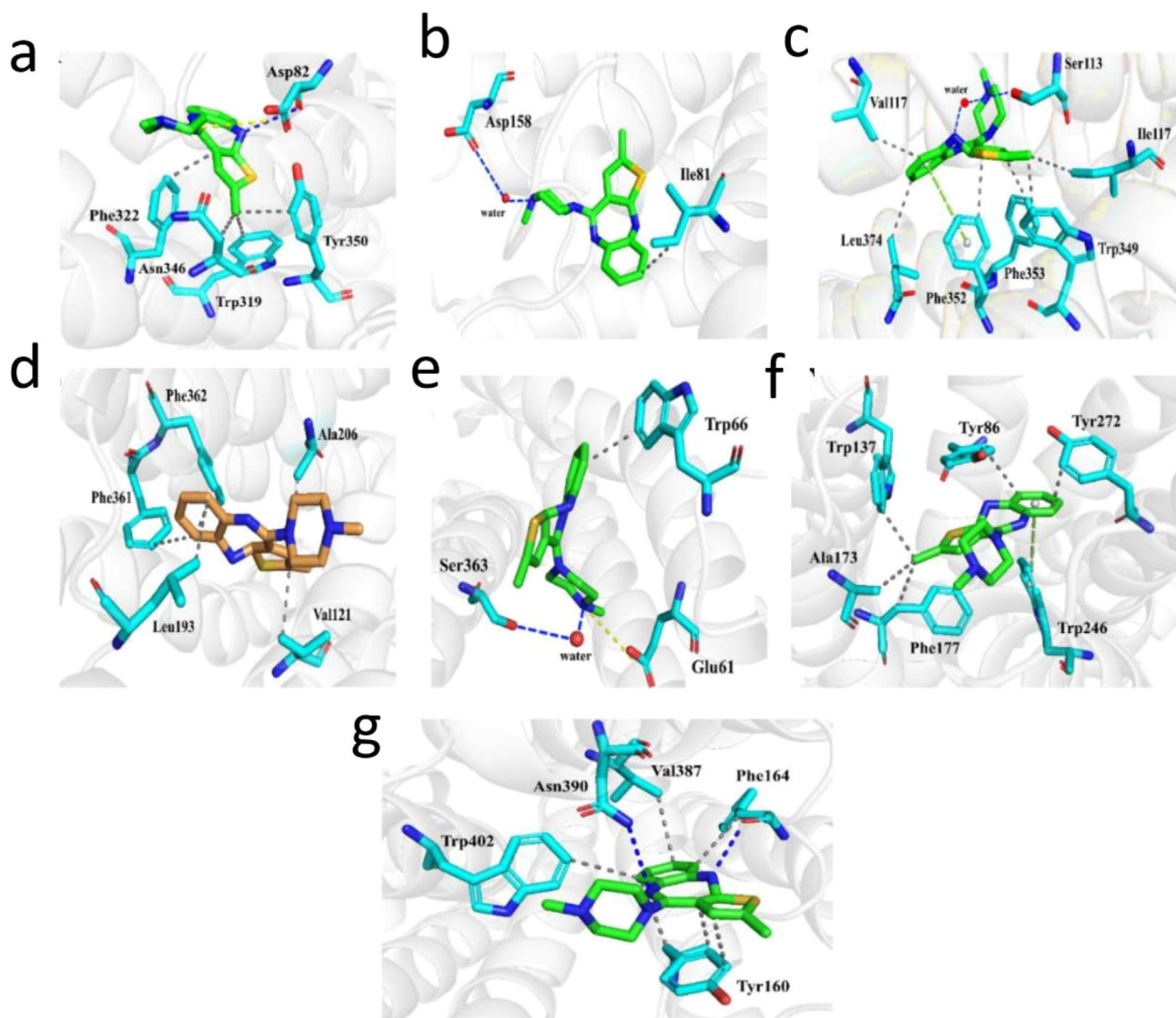
Figure 10. Ligand interactions of olanzapine and representative structure of (a) 5HT1A, (b) 5HT2A, (c) 5HT2B, (d) 5HT2C, (e) DRD2, (f) CHRM1, and (g) CHRM2 obtained from cluster analysis.

Likewise, in cluster analysis, we investigated how the ligand is located in the active site of the proteins and interacts with important residues after 300 ns molecular dynamics simulations. In the complex related to olanzapine ligand and 5HT1A (Figure 10) residue Asp82 with hydrogen bond interaction (as also observed in hydrogen bond analysis), and salt bridge, including Trp319, Phe322, Asn346, and Tyr350 had effective hydrophobic interactions with different parts of the ligand. Concerning the ligand being in the active site of the 5HT2A structure, these interactions involve residues Asp158, which forms a hydrogen bond with water and bridges the water between the residue and the ligand, and Ile81, which interacts with the ligand in a hydrophobic way.

It is important to form a hydrogen bond with water and bridge the water between the residue and the ligand to provide the residues Ser113, Val117, Phe352, Trp349, and Leu374 essential hydrophobic interactions in complex with the target 5HT2B. As shown in Figure 10, the green lines depict pi-pi stacking and important interactions. When olanzapine is present in the active site of 5HT2C, certain hydrophobic interactions between the residues; Val121, Leu193,

Ala206, Phe361, and Phe362 can be observed (Figure 10). Following and reviewing this analysis, residues from the dopamine D2 receptor structure thathad a clear interaction with the selected ligand; was a hydrophobic interaction with Trp66, a salt bridge between the selected ligand and Glu61, and finally, a hydrogen bond with water, bridging the water between the Ser363 and the ligand.

Several crucial residues interacted with the ligand in the active sites of the targets M1 and M2; depicted in Figure 10. . Hydrophobic interactions related to residues Tyr86, Trp137, Ala173, Phe177, and Tyr272 were related to target M1. In addition, hydrophobic interactions between Tyr160, Phe164, Val387, Asn390, and Trp402 including hydrogen bonds with Asn390 and Phe164 were observed with M2 (Figure 10).

Moreover, the safety limitations of the typical antipsychotics i.e. extrapyramidal syndromes, atypical antipsychotics have played an important role in the management of psychiatric illness and clinical psychopharmacology; olanzapine is one of the most common atypical anti-psychotics which has an important role in managing various psychiatric illnesses including major depression and schizophrenia; however, is
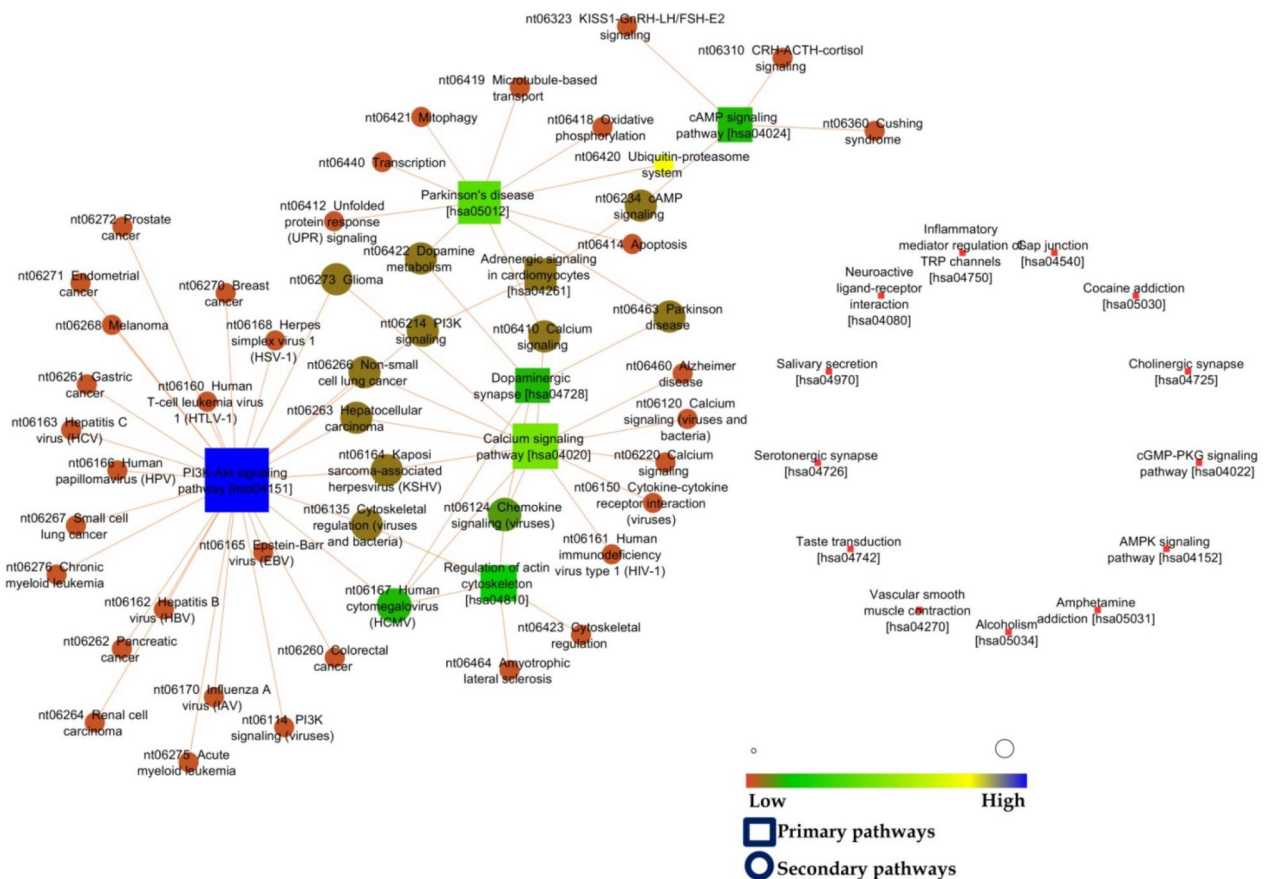
Figure 11. Network of olanzapine-modulated pathways with secondary pathways. serotonergic synapse; hsa04726, gap junction; hsa04540, alcoholism; hsa05034, amphetamine addiction; hsa05031, taste transduction; hsa04742, cGMP-PKG signaling pathway; hsa04022, inflammatory mediator regulation of TRP channels; hsa04750, cholinergic synapse; hsa04725, cocaine addiction; hsa05030, salivary secretion; hsa04970, neuroactive ligand-receptor interaction; hsa04080, AMPK signaling pathway; hsa04152, and vascular smooth muscle contraction hsa04270 were not networked with any secondary pathways.

associated with metabolic disorders (Li et al., 2019). Among them, olanzapine-induced weight gain has been recorded as a critical observation in subjects under the pharmacotherapy of olanzapine (Guha et al., 2005) which is also demonstrated in an experimental animal model of rats (Fernø et al., 2011; Li et al., 2019; Ullagaddi et al., 2021) and zebrafish (Khanal et al., 2020).

The management of psychiatric illness with olanzapine-pharmacotherapy is based on its antagonistic effect on various G-protein coupled receptors i.e. dopamine 2 receptors followed by multiple subunits of adrenergic and serotonin receptors including histamine (Olanzapine; https://go.drug-bank.com/drugs/DB00334). These surface G-protein coupled receptors are predominantly available at the satiety center and are involved in the regulation of appetite and homeostatic energy expenditure (Avena & Rada, 2012; Cassidy & Tong, 2017; Provensi et al., 2016; Voigt & Fink, 2015). Also, a record has been made for the antagonistic effect of olanzapine over histamine, serotonin, and muscarinic receptor (Olanzapine; https://go.drugbank.com/drugs/DB00334). Supporting previous reports, in the present study, we observed, that the majority of the receptors modulated by olanzapine were under the category of the G-protein coupled receptor majorly targeting the serotonin, histamine, adrenergic, and muscarinic receptor subunits. This observation suggests that olanzapine-induced hyperphagia could be

associated with the antagonistic effect of the olanzapine over the various neurotransmitter synapses which are also supported via the regulation of neuroactive ligand-receptor interaction as it represents the variety of signaling molecules including many types of neuroreceptor. Also, the regulation of food consumption is regulated via taste transduction which is managed by the reward and feeding center which is closely associated with the dopamine regulatory system (Volkow et al., 2011). In the present study, we observed the regulation of the dopamine synapse which may have contributed to the taste transduction as identified in the present study.

Another theory for olanzapine-induced weight gain includes the concept of compromised energy expenditure which is demonstrated in various animal models via loco-motor activity (Ullagaddi et al., 2021). The energy expenditure in homeostasis is regulated by multiple pathways like cGMP-PKG (Francis et al., 2010), PI3K-Akt (Lin et al., 2010), and AMPK (Hardie et al., 2012) signaling pathways. In olanzapine-induced obesity, previously it has been commented that the deposition of the white adipose tissue increased (Babic et al., 2021). One of the studies suggested that the upregulation of the cGMP level promotes the development of the brown adipose tissue to dissipate the energy as non-severing thermogenesis (Pfeifer et al., 2013). In the present study, we observed the regulation of the cGMP pathway via

the combined interaction of the olanzapine-regulated targets triggered by muscarinic 1 and 2, dopamine 1 and 2, and serotonin 1 subunit receptors. Thus, it can be further speculated that high deposition of the free fatty acids and white fat deposition in olanzapine-induced obesity could be cGMP-PKG-mediated.

Mild hyperglycaemic state and elevated blood pressure have been reported in subjects under the long-term pharmacotherapy of olanzapine which is also demonstrated in the experimental animal models (Patil et al., 2006). Previously, archetype cAMP has been considered as a vital cellular signaling molecule to regulate the glucagon and insulin secretion from pancreatic α-and β-cells respectively; is considered as an amplifier of insulin secretion triggered via the Ca^{2+} in β-cells (Tengholm & Gylfe, 2017). Also, the antagonistic effect of olanzapine over the adrenergic, muscarinic, serotonin, and dopamine receptors may downregulate the calcium signaling pathway (KEGG entry: hsa04020) and alter the secretion of insulin from pancreatic β-cells as observed in the present study. Likewise, cAMP signaling-mediated downstream of cAMP has been reported for vasoconstriction in spontaneously hypertensive rats (Berg et al., 2009). Hence, reported the mild hyperglycaemic and hypertensive state with olanzapine treatment (Patil et al., 2006) could be due to cAMP pathway mediated; triggered via the regulation of HTR6, CHRM1, HTR1A, DRD2, DRD1, CHRM2.

PI3K-Akt signaling pathway has been well documented for the upregulation of the lipid biosynthesis and downregulation of lipolysis which is regulated by SREBP; regulator of fatty acid synthase and FOXO1; regulates the expression of the adipose triglyceride lipase, are considered as the substrates for AKT-metabolism (Huang et al., 2018). Additionally, β-adrenergic signaling upregulates acute lipolysis with cAMP accumulation (Mottillo & Granneman, 2011) which was predicted to be affected by the olanzapine as discussed above. In the present findings, olanzapine was identified to act over the prolactin and muscarinic 1 and 2 receptors and alter the function of the PI3K-Akt pathway; this could be the reason for a dyslipidaemic profile in olanzapine-associated weight gain. The modulation of thermogenesis in adipose tissue has been used to pinpoint the AMPK signaling pathway as the controlling mechanism of energy metabolism. Also, it regulates the browning process of inguinal white adipose tissue and maintains energy homeostasis (Wu et al., 2018). The homeostatic function of the AMPK signaling pathway, which may have been activated by the ADRA1A and ADIPOQ and affect the thermogenic regulation of energy expenditure, was impacted in the current study.

In addition, three gene ontology terms i.e. molecular function, biological process, and cellular components define how the combinatorial interactions of numerous proteins are regulated by a single substance or multiple compounds. This complex effect could act over the multiple proteins/genes and trigger the multiple pathways for various pharmacological spectra and regulate multiple secondary pathways (Figure 11) which needs to be further investigated. However, based on the assessment of the combined action of the regulated proteins and pathways, it can be predicted that olanzapine can act over the multiple proteins preferably G-protein coupled receptors, affect the synapse of the multiple receptors and upregulate the feeding center and inhibit the thermogenesis via its action over cGMP-PKG, cAMP, and PI3K-Akt signaling pathway and taste transduction.

Conclusion

The present study utilized the multiple system biology tools to investigate the olanzapine-induced metabolic pathways that are primarily involved in glucose and lipid homeostasis which identified the deregulation of the multiple synapse and cGMP-PKG, cAMP, and PI3K-Akt signaling pathway. In addition, the binding affinity of the olanzapine ligand with different surface proteins was discussed. After performing 300 ns molecular dynamics simulations and various analyses, the amount of binding energy was used to achieve the free energy from the MMPBSA/MMGBSA process, which was an accurate ligand rating methodology. To evaluate the metabolic pathways linked to the weight gain associated with olanzapine, an appropriate wet lab experiment is required to validate the findings of the current investigation with a focus on reported synapses followed by cGMP-PKG, cAMP, and PI3K-Akt signaling pathways.

Ethical approval

This work doesn't include any human participation or animals to retrieve data.

Disclosure statement

The authors of this manuscript declare that they do not possess any financial or non-financial conflict of interest related to this manuscript. All authors of this manuscript have read and approved the manuscript for submission.

ORCID

Pukar Khanal (iD) http://orcid.org/0000-0002-8187-2120
Yadu Nandan Dey (iD) http://orcid.org/0000-0003-4016-4379

Author contribution

Pukar Khanal: Generated a concept of tracing the olanzapine-associated metabolic pathways in obesity using network biology and experimented on functional enrichment analysis and drafted the first manuscript. **Farshid Zargari** and **Zahra Nikfarjam**: Contributed to the molecular docking and molecular dynamics simulation study. **Yadu Nandan Dey**: Supervised the entire work, and manuscript draft, edited, and reviewed.

References

Albaugh, V. L., Henry, C. R., Bello, N. T., Hajnal, A., Lynch, S. L., Halle, B., & Lynch, C. J. (2006). Hormonal and metabolic effects of olanzapine and clozapine related to body weight in rodents. *Obesity*, 14(1), 36–51. https://doi.org/10.1038/oby.2006.6

Avena, N. M., & Rada, P. V. (2012). Cholinergic modulation of food and drug satiety and withdrawal. *Physiology & Behavior*, 106(3), 332–336. https://doi.org/10.1016/j.physbeh.2012.03.020

Babic, I., Sellers, D., Else, P. L., Nealon, J., Osborne, A. L., Pai, N., & Weston-Green, K. (2021). Effect of liraglutide on neural and peripheral markers of metabolic function during antipsychotic treatment in rats. *Journal of Psychopharmacology*, 35(3), 284–302. https://doi.org/10.1177/0269881120981377

Ben-Shalom, I. Y., Pfeiffer-Marek, S., Baringhaus, K. H., & Gohlke, H. (2017). Efficient approximation of ligand rotational and translational entropy changes upon binding for use in MM-PBSA calculations. *Journal of Chemical Information and Modeling*, 57(2), 170–189. https://doi.org/10.1021/acs.jcim.6b00373

Berg, T., Degerman, E., & Tasken, K. (2009). Increased cAMP signaling can ameliorate the hypertensive condition in spontaneously hypertensive rats. *Journal of Vascular Research*, 46(1), 25–35. https://doi.org/10.1159/000135662

Case, D. A., Aktulga, H. M., Belfon, K., Ben-Shalom, I. Y., Berryman, J. T., Brozell, S. R., Cerutti, D. S., Cheatham, T. E., Cisneros, G. A., Cruzeiro, V. W. D., Darden, T. A., Duke, R. E., Giambasu, G., Gilson, M. K., Gohlke, H., Goetz, A. W., Harris, R., Izadi, S., Izmailov, S. A., … Kollman, P. A. (2022). Amber 2022, University of California, San Francisco. https://ambermd.org/index.php

Cassidy, R. M., & Tong, Q. (2017). Hunger and satiety gauge reward sensitivity. *Frontiers in Endocrinology*, 8, 104. https://doi.org/10.3389/fendo.2017.00104

Chang, S., Zhang, D. W., Xu, L., Wan, H., Hou, T. J., & Kong, R. (2016). Exploring the molecular basis of RNA recognition by the dimeric RNA-binding protein via molecular simulation methods. *RNA Biology*, 13(11), 1133–1143. https://doi.org/10.1080/15476286.2016.1223007

De Paris, R., Quevedo, C. V., Ruiz, D. D., Norberto de Souza, O., & Barros, R. C. (2015). Clustering molecular dynamics trajectories for optimizing docking experiments. *Computational Intelligence and Neuroscience*, 2015, 916240. https://doi.org/10.1155/2015/916240

Duan, L., Liu, X., & Zhang, J. Z. (2016). Interaction Entropy: A New Paradigm for Highly Efficient and Reliable Computation of Protein-Ligand Binding Free Energy. *Journal of the American Chemical Society*, 138(17), 5722–5728. https://doi.org/10.1021/jacs.6b02682

Feig, M., Onufriev, A., Lee, M. S., Im, W., Case, D. A., & Brooks, C. L. 3rd (2004). Performance comparison of generalized born and Poisson methods in the calculation of electrostatic solvation energies for protein structures. *Journal of Computational Chemistry*, 25(2), 265–284. https://doi.org/10.1002/jcc.10378

Fernø, J., Varela, L., Skrede, S., Vázquez, M. J., Nogueiras, R., Diéguez, C., Vidal-Puig, A., Steen, V. M., & López, M. (2011). Olanzapine-induced hyperphagia and weight gain associate with orexigenic hypothalamic neuropeptide signaling without concomitant AMPK phosphorylation. *PLoS One*, 6(6), e20571. https://doi.org/10.1371/journal.pone.0020571

Fiser, A., Do, R. K., & Sali, A. (2000). Modeling of loops in protein structures. *Protein Science*, 9(9), 1753–1773. https://doi.org/10.1110/ps.9.9.1753

Foloppe, N., & Hubbard, R. (2006). Towards predictive ligand design with free-energy based computational methods? *Current Medicinal Chemistry*, 13(29), 3583–3608. https://doi.org/10.2174/092986706779026165

Francis, S. H., Busch, J. L., Corbin, J. D., & Sibley, D. (2010). cGMP-dependent protein kinases and cGMP phosphodiesterases in nitric oxide and cGMP action. *Pharmacological Reviews*, 62(3), 525–563. https://doi.org/10.1124/pr.110.002907

Genheden, S., Akke, M., & Ryde, U. (2014). Conformational Entropies and Order Parameters: Convergence, Reproducibility, and Transferability. *Journal of Chemical Theory and Computation*, 10(1), 432–438. https://doi.org/10.1021/ct400747s

Genheden, S., Kuhn, O., Mikulskis, P., Hoffmann, D., & Ryde, U. (2012). The normal-mode entropy in the MM/GBSA method: Effect of system truncation, buffer region, and dielectric constant. *Journal of Chemical Information and Modeling*, 52(8), 2079–2088. https://doi.org/10.1021/ci3001919

Genheden, S., & Ryde, U. (2012). Will molecular dynamics simulations of proteins ever reach equilibrium? *Physical Chemistry Chemical Physics : PCCP*, 14(24), 8662–8677. https://doi.org/10.1039/c2cp23961b

Gfeller, D., Grosdidier, A., Wirth, M., Daina, A., Michielin, O., & Zoete, V. (2014). SwissTargetPrediction: A web server for target prediction of bioactive small molecules. *Nucleic Acids Research*, 42(Web Server issue), W32–W38. https://doi.org/10.1093/nar/gku293

Guha, P., Roy, K., Sanyal, D., Dasgupta, T., & Bhattacharya, K. (2005). Olanzapine-induced obesity and diabetes in Indian patients: A prospective trial comparing olanzapine with typical antipsychotics. *Journal of the Indian Medical Association*, 103(12), 660–664.

Hardie, D. G., Ross, F. A., & Hawley, S. A. (2012). AMPK: A nutrient and energy sensor that maintains energy homeostasis. *Nature Reviews. Molecular Cell Biology*, 13(4), 251–262. https://doi.org/10.1038/nrm3311

Hou, T., & Yu, R. (2007). Molecular dynamics and free energy studies on the wild-type and double mutant HIV-1 protease complexed with amprenavir and two amprenavir-related inhibitors: Mechanism for binding and drug resistance. *Journal of Medicinal Chemistry*, 50(6), 1177–1188. https://doi.org/10.1021/jm0609162

Hu, Y., Young, A. J., Ehli, E. A., Nowotny, D., Davies, P. S., Droke, E. A., Soundy, T. J., & Davies, G. E. (2014). Metformin and berberine prevent olanzapine-induced weight gain in rats. *PloS One*, 9(3), e93310. https://doi.org/10.1371/journal.pone.0093310

Huang, X., Liu, G., Guo, J., & Su, Z. (2018). The PI3K/AKT pathway in obesity and type 2 diabetes. *International Journal of Biological Sciences*, 14(11), 1483–1496. https://doi.org/10.7150/ijbs.27173

Izadi, S., Anandakrishnan, R., & Onufriev, A. V. (2014). Building Water Models: A Different Approach. *The Journal of Physical Chemistry Letters*, 5(21), 3863–3871. https://doi.org/10.1021/jz501780a

Jin, Z., Du, X., Xu, Y., Deng, Y., Liu, M., Zhao, Y., Zhang, B., Li, X., Zhang, L., Peng, C., Duan, Y., Yu, J., Wang, L., Yang, K., Liu, F., Jiang, R., Yang, X., You, T., Liu, X., … Yang, H. (2020). Structure of Mpro from SARS-CoV-2 and discovery of its inhibitors. *Nature*, 582(7811), 289–293. https://doi.org/10.1038/s41586-020-2223-y

Jo, S., Kim, T., Iyer, V. G., & Im, W. (2008). CHARMM-GUI: A web-based graphical user interface for CHARMM. *Journal of Computational Chemistry*, 29(11), 1859–1865. https://doi.org/10.1002/jcc.20945

Kiani, Y. S., Ranaghan, K. E., Jabeen, I., & Mulholland, A. J. (2019). Molecular Dynamics Simulation Framework to Probe the Binding Hypothesis of CYP3A4 Inhibitors.*International Journal of Molecular Sciences*, 20(18), 4468. https://doi.org/10.3390/ijms20184468

Khanal, P., Patil, B. M., & Unger, B. S. (2020). Zebrafish shares common metabolic pathways with mammalian olanzapine-induced obesity. *Future Journal of Pharmaceutical Sciences*, **6**(1), 36. https://doi.org/10.1186/s43094-020-00049-7

Lagunin, A., Ivanov, S., Rudik, A., Filimonov, D., & Poroikov, V. (2013). DIGEP-Pred: Web service for in silico prediction of drug-induced gene expression profiles based on structural formula. *Bioinformatics*, 29(16), 2062–2063. https://doi.org/10.1093/bioinformatics/btt322

Li, H., Peng, S., Li, S., Liu, S., Lv, Y., Yang, N., Yu, L., Deng, Y. H., Zhang, Z., Fang, M., Huo, Y., Chen, Y., Sun, T., & Li, W. (2019). Chronic olanzapine administration causes metabolic syndrome through inflammatory cytokines in rodent models of insulin resistance. *Scientific Reports*, 9(1), 1582. https://doi.org/10.1038/s41598-018-36930-y

Lin, J., Wang, J., Greisinger, A. J., Grossman, H. B., Forman, M. R., Dinney, C. P., Hawk, E. T., & Wu, X. (2010). Energy balance, the PI3K-AKT-mTOR pathway genes, and the risk of bladder cancer. *Cancer Prevention Research*, 3(4), 505–517. https://doi.org/10.1158/1940-6207.CAPR-09-0263

Liu, N., & Xu, Z. (2019). Using LeDock as a docking tool for computational drug designIOP Conf. *Series: Earth and Environmental Science*, 218, 012143.

Liu, T., Lin, Y., Wen, X., Jorissen, R. N., & Gilson, M. K. (2007). BindingDB: A web-accessible database of experimentally determined protein-ligand binding affinities. *Nucleic Acids Research*, 35(Database issue), D198–D201. https://doi.org/10.1093/nar/gkl999

Lomize, M. A., Pogozheva, I. D., Joo, H., Mosberg, H. I., & Lomize, A. L. (2012). OPM database and PPM web server: Resources for positioning of proteins in membranes. *Nucleic Acids Research*, *40*(Database issue), D370–D376. https://doi.org/10.1093/nar/gkr703

Lord, C. C., Wyler, S. C., Wan, R., Castorena, C. M., Ahmed, N., Mathew, D., Lee, S., Liu, C., & Elmquist, J. K. (2017). The atypical antipsychotic olanzapine causes weight gain by targeting serotonin receptor 2C. *The Journal of Clinical Investigation*, *127*(9), 3402–3406. https://doi.org/10.1172/JCI93362

Martí-Renom, M. A., Stuart, A. C., Fiser, A., Sánchez, R., Melo, F., & Sali, A. (2000). Comparative protein structure modeling of genes and genomes. *Annual Review of Biophysics and Biomolecular Structure*, *29*, 291–325. https://doi.org/10.1146/annurev.biophys.29.1.291

Mottillo, E. P., & Granneman, J. G. (2011). Intracellular fatty acids suppress β-adrenergic induction of PKA-targeted gene expression in white adipocytes. *American Journal of Physiology. Endocrinology and Metabolism*, *301*(1), E122–E131. https://doi.org/10.1152/ajpendo.00039.2011

Morris, G. M., & Lim-Wilby, M. (2008). Molecular docking. *Methods in Molecular Biology (Clifton, N.J.)*, *443*, 365–382. https://doi.org/10.1007/978-1-59745-177-2

Narasimhan, M., Bruce, T. O., & Masand, P. (2007). Review of olanzapine in the management of bipolar disorders. *Neuropsychiatric Disease and Treatment*, *3*(5), 579–587.

Nikfarjam, Z., Bavi, O., & Amini, S. K. (2021). Potential effective inhibitory compounds against Prostate Specific Membrane Antigen (PSMA): A molecular docking and molecular dynamics study. *Archives of Biochemistry and Biophysics*, *699*, 108747. https://doi.org/10.1016/j.abb.2020.108747

Oliveros, J. C. (2007–2015). Venny. An interactive tool for comparing lists with Venn's diagrams. https://bioinfogp.cnb.csic.es/tools/venny/index.html

Parasuraman, S., Zhen, K. M., Banik, U., & Christapher, P. V. (2017). Ameliorative Effect of Curcumin on Olanzapine-induced Obesity in Sprague-Dawley Rats. *Pharmacognosy Research*, *9*(3), 247–252. https://doi.org/10.4103/pr.pr_8_17

Patil, B. M., Kulkarni, N. M., & Unger, B. S. (2006). Elevation of systolic blood pressure in an animal model of olanzapine induced weight gain. *European Journal of Pharmacology*, *551*(1-3), 112–115. https://doi.org/10.1016/j.ejphar.2006.09.009

Pettersen, E. F., Goddard, T. D., Huang, C. C., Couch, G. S., Greenblatt, D. M., Meng, E. C., & Ferrin, T. E. (2004). UCSF Chimera–a visualization system for exploratory research and analysis. *Journal of Computational Chemistry*, *25*(13), 1605–1612. https://doi.org/10.1002/jcc.20084

Pfeifer, A., Kilić, A., & Hoffmann, L. (2013). Role of cGMP in fat and metabolism. *BMC Pharmacology and Toxicology*, *14*(S1), O25. https://doi.org/10.1186/2050-6511-14-S1-O25

Piñero, J., Bravo, À., Queralt-Rosinach, N., Gutiérrez-Sacristán, A., Deu-Pons, J., Centeno, E., García-García, J., Sanz, F., & Furlong, L. I. (2017). DisGeNET: A comprehensive platform integrating information on human disease-associated genes and variants. *Nucleic Acids Research*, *45*(D1), D833–D839. https://doi.org/10.1093/nar/gkw943

Provensi, G., Blandina, P., & Passani, M. B. (2016). The histaminergic system as a target for the prevention of obesity and metabolic syndrome. *Neuropharmacology*, *106*, 3–12. https://doi.org/10.1016/j.neuropharm.2015.07.002

Sali, A., & Blundell, T. L. (1993). Comparative protein modelling by satisfaction of spatial restraints. *Journal of Molecular Biology*, *234*(3), 779–815. https://doi.org/10.1006/jmbi.1993.1626

Shahraki, O., Zargari, F., Edraki, N., Khoshneviszadeh, M., Firuzi, O., & Miri, R. (2018). Molecular dynamics simulation and molecular docking studies of 1,4-Dihydropyridines as P-glycoprotein's allosteric inhibitors. *Journal of Biomolecular Structure & Dynamics*, *36*(1), 112–125. https://doi.org/10.1080/07391102.2016.1268976

Shannon, P., Markiel, A., Ozier, O., Baliga, N. S., Wang, J. T., Ramage, D., Amin, N., Schwikowski, B., & Ideker, T. (2003). Cytoscape: A software environment for integrated models of biomolecular interaction networks. *Genome Research*, *13*(11), 2498–2504. https://doi.org/10.1101/gr.1239303

Srinivasan, J., Trevathan, M. W., Beroza, P., & Case, D. A. (1999). Application of a pairwise generalized Born model to proteins and nucleic acids: Inclusion of salt effects. *Theoretical Chemistry Accounts*, *101*(6), 426–434. https://doi.org/10.1007/s002140050460

Sun, H., Duan, L., Chen, F., Liu, H., Wang, Z., Pan, P., Zhu, F., Zhang, J., & Hou, T. (2018). Assessing the performance of MM/PBSA and MM/GBSA methods. 7. Entropy effects on the performance of end-point binding free energy calculation approaches. *Physical Chemistry Chemical Physics : PCCP*, *20*(21), 14450–14460. https://doi.org/10.1039/c7cp07623a

Sun, H. Y., Ji, F. Q., Fu, L. Y., Wang, Z. Y., & Zhang, H. Y. (2013). Structural and energetic analyses of SNPs in drug targets and implications for drug therapy. *Journal of Chemical Information and Modeling*, *53*(12), 3343–3351. https://doi.org/10.1021/ci400457v

Swanson, J. M., Henchman, R. H., & McCammon, J. A. (2004). Revisiting free energy calculations: A theoretical connection to MM/PBSA and direct calculation of the association free energy. *Biophysical Journal*, *86*(1 Pt 1), 67–74. https://doi.org/10.1016/S0006-3495(04)74084-9

Szklarczyk, D., Gable, A. L., Lyon, D., Junge, A., Wyder, S., Huerta-Cepas, J., Simonovic, M., Doncheva, N. T., Morris, J. H., Bork, P., Jensen, L. J., & Mering, C. V. (2019). STRING v11: Protein-protein association networks with increased coverage, supporting functional discovery in genome-wide experimental datasets. *Nucleic Acids Research*, *47*(D1), D607–D613. https://doi.org/10.1093/nar/gky1131

Tengholm, A., & Gylfe, E. (2017). cAMP signalling in insulin and glucagon secretion. *Diabetes, Obesity and Metabolism*, *19*(Suppl 1), 42–53. https://doi.org/10.1111/dom.12993

Ullagaddi, M. B., Patil, B. M., & Khanal, P. (2021). Beneficial effect of *Zingiber officinale* on olanzapine-induced weight gain and metabolic changes. *Journal of Diabetes and Metabolic Disorders*, *20*(1), 41–48. https://doi.org/10.1007/s40200-020-00695-x

VARGiu, A. V., & Magistrato, A. (2012). Detecting DNA mismatches with metallo-insertors: A molecular simulation study. *Inorganic Chemistry*, *51*(4), 2046–2057. https://doi.org/10.1021/ic201659v

Voigt, J. P., & Fink, H. (2015). Serotonin controlling feeding and satiety. *Behavioural Brain Research*, *277*, 14–31. https://doi.org/10.1016/j.bbr.2014.08.065

Volkow, N. D., Wang, G. J., & Baler, R. D. (2011). Reward, dopamine and the control of food intake: Implications for obesity. *Trends in Cognitive Sciences*, *15*(1), 37–46. https://doi.org/10.1016/j.tics.2010.11.001

Wang, C., Nguyen, P. H., Pham, K., Huynh, D., Le, T. B., Wang, H., Ren, P., & Luo, R. (2016). Calculating protein-ligand binding affinities with MMPBSA: Method and error analysis. *Journal of Computational Chemistry*, *37*(27), 2436–2446. https://doi.org/10.1002/jcc.24467

Wang, W., Donini, O., Reyes, C. M., & Kollman, P. A. (2001). Biomolecular simulations: Recent developments in force fields, simulations of enzyme catalysis, protein-ligand, protein-protein, and protein-nucleic acid noncovalent interactions. *Annual Review of Biophysics and Biomolecular Structure*, *30*, 211–243. https://doi.org/10.1146/annurev.biophys.30.1.211

Wu, L., Zhang, L., Li, B., Jiang, H., Duan, Y., Xie, Z., Shuai, L., Li, J., & Li, J. (2018). AMP-Activated Protein Kinase (AMPK) Regulates Energy Metabolism through Modulating Thermogenesis in Adipose Tissue. *Frontiers in Physiology*, *9*, 122. https://doi.org/10.3389/fphys.2018.00122